HHS Public Access

Author manuscript

J Neurol Neurosurg Psychiatry. Author manuscript; available in PMC 2023 October 23.

Published in final edited form as:

J Neurol Neurosurg Psychiatry. 2022 April ; 93(4): 386–394. doi:10.1136/jnnp-2021-326962.

Motor context modulates substantia nigra pars reticulata spike activity in patients with Parkinson's disease

Anand Tekriwal[*,1,2,3,4], **Gidon Felsen**[2,3,4], **Steven Ojemann**[1], **Aviva Abosch**[5], **John A. Thompson**[1,2,3,4,6]

[1]Department of Neurosurgery, University of Colorado School of Medicine, Aurora, CO 80045

[2]Department of Physiology and Biophysics, University of Colorado School of Medicine, Aurora, CO 80045

[3]Neuroscience Graduate Program, University of Colorado School of Medicine, Aurora, CO 80045

[4]Medical Scientist Training Program, University of Colorado School of Medicine, Aurora, CO 80045

[5]Department of Neurosurgery, University of Nebraska Medical Center, Omaha, NE 68198

[6]Department of Neurology, University of Colorado School of Medicine, Aurora, CO 80045

Abstract

Objectives: The severity of motor symptoms in Parkinson's disease (PD) depends on environmental conditions. For example, the presence of external patterns such as a rhythmic tone can attenuate bradykinetic impairments. However, the neural mechanisms for this context-dependent attenuation remain unknown. Here, we investigate whether context-dependent symptom attenuation is reflected in single-unit activity recorded in the operating room from the substantia nigra pars reticulata (SNr) of PD patients undergoing deep brain stimulation surgery (DBS). The SNr is known to influence motor planning and execution in animal models but its role in humans remains understudied.

Methods: We recorded SNr activity while subjects performed cued directional movements in response to auditory stimuli under interleaved "patterned" and "unpatterned" contexts. SNr localization was independently confirmed with expert intraoperative assessment as well as post-hoc imaging-based reconstructions.

[*]To whom correspondence should be addressed andy.tekriwal@cuanschutz.edu, Department of Neurosurgery and Department of Physiology & Biophysics, University of Colorado Anschutz Medical Campus, 12800 E. 19th Ave., Mail Stop 8307, Aurora, CO 80045, USA.

Contributions :

Authors AT, GF, and JT designed the experiment with AT, SGO, AA, and JT carrying out data collection. Electrophysiologic and behavioral analyses were performed by AT and post-hoc imaging verification by JT. Text and figures were created by AT with significant input from all other authors, especially JT.

Competing interests:

Authors declare no competing interests.

Ethics approval:

Study approval was granted by the Colorado Multiple Institutional Review Board (Protocol#:17-1291) and informed consent was attained for all study participants.

Results: As predicted, we found that motor performance was improved in the patterned context, reflected in increased reaction speed and accuracy compared to the unpatterned context. These behavioral differences were associated with enhanced responsiveness of SNr neurons – i.e., larger changes in activity from baseline – in the patterned context. Unsupervised clustering analysis revealed two distinct subtypes of SNr neurons: one exhibited context-dependent enhanced responsiveness exclusively during movement preparation, whereas the other showed enhanced responsiveness during portions of the task associated with both motor and non-motor processes.

Conclusions: Our findings indicate the SNr serves roles in motor planning and execution, as well as warrants greater attention in the study of human sensorimotor integration and as a target for neuromodulatory therapies.

Keywords

Human electrophysiology; Intraoperative; Parkinson's disease; Basal ganglia; GABAergic

Introduction

Parkinson's disease (PD) is a movement disorder typified by resting tremor, bradykinesia, limb rigidity, and postural instability. The motor manifestations of PD arise from the degeneration of dopamine-secreting (DA) neurons in the SNc (substantia nigra pars compacta), leading to dysregulation of SNc targets which include the SNr (substantia nigra pars reticulata) through direct and indirect projections [1 2]. The SNr is an important basal ganglia (BG) output structure with direct GABAergic projections to thalamic and pontomesencephalic nuclei. Animal model findings indicate these circuits are implicated in motor integration, planning and execution [1 3-7], but their functional significance in humans and human disease remains severely understudied [8-13]. Here we test the clinically relevant hypothesis that parkinsonian symptoms, such as bradykinesia, are modulated by context and by extension that BG output is responsive to the presence of patterned stimuli in the environment. Prior studies have demonstrated that-sensory cues can significantly improve ambulation speed and balance of patients with PD; however, little is known of the neural basis for this context dependence [14-18]. Given known BG involvement in mediating habitual motor behaviors, we posit that differentiable SNr activity patterns may underlie context dependent modulation of PD symptoms.

To test this hypothesis, we recorded SNr single neuron responses from awake behaving subjects in the operating room during an auditory cued decision-making task [19] designed to simulate two different contextual conditions: "patterned" or "unpatterned" (Methods, Fig. 1B). The overall structure of trials in each condition were identical with the only difference being the predictability of stimulus-response pairings. During unpatterned blocks of trials, subjects were presented with a variety of auditory tones (one per trial) and instructed to make leftward movements for low-pitch tones and rightward movements for high-pitch tones (Fig. 1B,C (left)). In contrast, in patterned blocks of trials the presented stimulus was consistently a neutral, mid-pitch tone, with the correct movement responses fixed to one side for the duration of the block (Fig. 1B,C (right)). In line with our predictions (Fig. 1D), the stable sequence of stimulus-response pairings in the patterned context led to an attenuation of bradykinetic symptoms and allowed us to examine the context-dependence of

SNr activity. Leveraging the identical task structure of patterned and unpatterned trials, we examined how SNr activity changed in each of five, sequential epochs defined based on task events (Fig. 3A).

We found that activity within a given epoch significantly deviated from baseline in an epoch-specific manner, indicating SNr activity is sensitive to trial time course and underlying demands. When analyzing within-epoch activity changes, significant contextual and directional effects on firing rate were revealed (Fig. 3, Supplementary Materials and Methods). Specifically, we observed larger changes from baseline under the patterned condition for *sensory processing, movement preparation*, and *movement initiation* epochs (Fig. 4A), as well as across all epochs when controlling for direction of movement (Fig. 4C). Building off these interesting findings we next used machine learning tools to determine whether subtypes of SNr neurons lent specific contributions to our population level findings. Characterizing using waveform features, we found subtypes with distinct SNr functional profiles for the first time in humans [20 21], that when combined largely accounted for population level findings (Fig. 5). Taken together, these findings make several unique contributions to our understanding of PD effected BG physiology: 1) human SNr neurons demonstrate contextual and directional responsiveness 2) context strongly influences SNr output during pre and peri-movement epochs and 3) subtypes of SNr neurons show related but non-overlapping functional profiles.

Methods summary

Study participants

We collected intraoperative electrophysiological recordings from 9 subjects (4 male, Table 1) recruited at the University of Colorado Anschutz Medical Campus through the Movement Disorders Center from the population of adult patients undergoing deep brain stimulation (DBS) surgery for treatment of PD. Surgical candidacy was assessed by a clinical panel composed of representatives from neuropsychology, neurology, neuroradiology and neurosurgery. The mean age of patients at the time of the intraoperative study was 64 ± 7 years (± SD (standard deviation)) with PD duration of 11 ± 3 years. Eight subjects were right-handed, and we conducted the study on a single hemisphere in seven subjects and bilateral hemispheres in two subjects (Table 1). Pre-operative PD severity was measured with MDS-UPDRS-III and for our study group the average percent different between ON/OFF PD medication was 46 ± 24 (%) (OFF-ON/OFF) with average pre-surgery LEDD (levodopa equivalent daily dose) of 1350 ± 640 mg (Table 1). Inclusion criteria included consensus approval from the Multidisciplinary DBS Conference to undergo STN DBS for the treatment of PD, subject provision of informed consent, and intact bilateral hearing. Our study was carried out in accordance with the Colorado Multiple Institution Review Board (COMIRB; #17-1291) and Declaration of Helsinki with written informed consent obtained from all study subjects. For all participants, written consent was received prior to surgical date and photocopies of their complete, signed consent were provided back to them.

For details on surgical procedures, auditory sensorimotor task, data processing please, and data availability please refer to Supplementary Materials and Methods.

Results

The patterned context enhances behavioral performance

Subjects performed a behavioral task requiring movements in response to auditory stimuli presented in patterned and unpatterned contexts (Fig. 1A-C, Supplementary Materials and Methods). We predicted that motor performance, for identical movements, would differ between contexts (Fig. 1D) due to motor symptom attenuation induced by the patterned condition. To examine this prediction, we assessed average response time and found significantly faster responses for patterned contexts ($p = 0.0092$, 1-tailed Wilcoxon signed rank test (paired) Fig. 1E). Consistent with this result, we found that subjects gave the correct directional response more often under the patterned compared to unpatterned contexts ($p = 0.0173$, 1-tailed two-sample t-test (paired), Fig. 1F), with correct responses above chance levels in both indicating task comprehension. On 10/11 sessions, subjects exhibited performance on patterned trials that was at least as fast and accurate as on unpatterned trials. Taken together, these findings support our prediction of a context-dependent state in which movements were executed faster and more accurately in the patterned condition and allowed us to examine the neural basis of this context-dependent behavior.

Epoch-based analyses show SNr activity is modulated by context

We next sought to determine whether behavioral differences between patterned and unpatterned contexts could be associated with changes in activity recorded from SNr neurons (Fig. 2, Supplemental). We first quantified mean firing rate across the whole trial (Fig. 3A) as a broad measure of SNr activity and found no differences between the patterned and unpatterned contexts ($p = 0.7104$, 2-tailed t-test (paired)). Similarly, whole trial comparisons yielded no differences between trials with correct and incorrect responses ($p = 0.140$, 2-tailed t-test (paired)) or ipsilateral and contralateral responses ($p = 0.858$, 2-tailed t-test (paired)); note that left and right responses were converted to ipsilateral and contralateral based on the recorded hemisphere (Table 1, Supplementary Materials and Methods). When controlling for response direction and comparing between contexts we again found no whole-trial differences (unpatterned ipsi. vs patterned ipsi., $p = 0.453$, unpatterned contra. vs patterned contra., $p = 0.588$, both 2-tailed t-test (paired)).

However, when we examined the activity of individual SNr neurons during behaviorally defined task epochs, (Fig. 3A, Supplementary Materials and Methods), we identified groups of SNr neurons with distinct functional profiles, indicated by changes in firing rate during discrete behavioral epochs. Epochs were defined as follows: (epoch name (start : end)): *Priors* (500ms preceding 'Up' engaged : onset of auditory stimulus) *Sensory processing* (onset of auditory stimulus : 300ms following start of auditory stimulus), *Movement preparation* (300ms following start of auditory stimulus : go-tone), *Movement initiation* (go-tone, response submitted), *Feedback* (response submission: 500ms following feedback delivery). Specifically, epoch based analyses were used to compare the effect directional movements (ipsilateral or contralateral) and context (patterned or unpatterned) had on firing rate. For example, the representative neuron in Fig. 3B-D shows ipsilateral direction preference (i.e., higher firing rates for ipsilateral than contralateral movements) on

unpatterned trials during the *priors* epoch (Fig. 3B) and contralateral direction preference on patterned trials across all epochs except *sensory processing* (Fig. 3C). Examination of direction preference (ipsilateral - contralateral firing rates) across epochs illustrated a larger change on patterned trials, perhaps indicating greater recruitment of this neuron under the patterned context (Fig. 3D). We therefore examined whether epoch specific firing rates depended on task variables across the collected population of SNr neurons.

We first examined how activity depended on context (patterned vs. unpatterned; Fig. 4A). We focused on the "responsiveness" of each neuron, defined as the average difference in firing rate between a specific epoch and baseline (Supplementary Materials and Methods; this measure was used because preceding population level analyses demonstrated baseline activity did not change between conditions). We found that responsiveness was modulated by context for three consecutive epochs: *sensory processing* ($p = 0.0311$, 1-tailed Wilcoxon signed rank test (paired), adjusted for multiple (n=5) comparisons; $p = 0.0231$, Cohen's $d = 0.364$, 1-tailed paired permutation test; all permutations tests used 100,000 iterations), *movement preparation* ($p = 0.0284$, 1-tailed Wilcoxon signed rank test (paired), adjusted for multiple (n=5) comparisons; $p = 0.0234$, Cohen's $d = 0.220$, 1-tailed paired permutation test), and *movement initiation* ($p = 0.0284$, 1-tailed Wilcoxon signed rank test (paired) adjusted for multiple (n=5) comparisons; $p = 0.00376$, Cohen's $d = -0.284$, 1-tailed paired permutation test). Note, 1-tailed tests were predicated on an a priori hypothesis that patterned contexts would result in a greater change from baseline than unpatterned; to further account for multiple comparisons a Benjamini-Hochberg correction was applied. Interestingly, in epochs preceding movement (i.e., *sensory processing, movement preparation*), firing rates decreased from baseline, more so in patterned than unpatterned trials, whereas during *movement initiation* firing rates increased from baseline, more so in patterned than unpatterned trials. Thus, consistent with the representative neuron shown in Fig. 3D, neural activity was more varied on patterned trials, likely indicating greater recruitment of the population.

We next examined how responsiveness depended on movement direction (ipsilateral vs. contralateral; Fig. 4B). Surprisingly, given previous work demonstrating direction selectivity in SNr neurons [4 22 23], we found that responsiveness did not depend on direction in any epoch. However, when we examined how responsiveness depended on both context and direction together, we found pronounced context dependence across all epochs during ipsilateral (*priors*, $p = 0.00740$; *sensory processing*, $p = 0.0164$; *movement preparation*, $p = 0.00610$; *movement initiation*, $p = 0.00610$; *feedback*, $p = 0.0164$, 1-tailed Wilcoxon signed rank test (paired) adjusted for multiple (n=5) comparisons; *priors*, $p = 0.0183$, Cohen's $d = 0.333$; *sensory processing*, $p = 0.0178$, Cohen's $d = 0.484$; *movement preparation*, $p = 0.00475$, Cohen's $d = 0.327$; *movement initiation*, $p = 0.000615$, Cohen's $d = -0.422$; *feedback*, $p = 0.0250$, Cohen's $d = -0.253$, 1-tailed paired permutation test; Fig. 4C) but not contralateral (Fig. 4D) responses. This all-epoch (Fig. 4C) or no-epoch (Fig. 4D) result is notable considering the lack of overall directional selectivity (Fig. 4B) and demonstrates profound context-dependence responsiveness specifically for ipsilateral trials.

To determine whether population effects were driven by consistent changes across all neurons or strong responses from a minority of neurons, we performed a within neuron

regression analysis with context, direction and outcome as predictor variables. Results confirmed population level comparisons as expected given the uniformity of paired relationships (i.e., similar slopes for lines connecting paired points in Fig. 4). Of the 33 neurons, nearly half (14/33) demonstrated no significant interactions in any of the five epochs. Of the remaining (19/33), nearly all (15/19) showed interactions limited to a single epoch, with directional selectivity during the *movement preparation* epoch (4/19) as the most common feature. A shared feature of the few neurons (4/33) with significant interactions across more than one epoch was outcome selectivity during the *feedback* epoch. Taken together, within-neuron regression findings did not reveal pronounced effects of either a specific predictor variable or effects confined to a particular epoch.

Neuronal subtypes make distinct contributions to overall population findings

Given recent evidence for distinct functional subpopulations of GABAergic neurons in the SNr [20 21], we asked whether specific subpopulations were responsible for the effects shown in Fig. 4. We applied several approaches (Supplementary Materials and Methods) to characterize subtypes based on waveform characteristics. Briefly, we clustered multi-dimensional waveform data using t-SNE to reduce waveform dimensions, using both k-means and DBSCAN to assess putative groupings. These methods consistently yielded two distinct subtypes, characterized by waveforms with a leading negative deflection and greater amplitude (subtype A) as compared to narrower wave width and lesser amplitude (subtype B) (Fig. 5A, Supplementary Materials and Methods). To further demonstrate robust cluster separation, we ran a non-PCA, linear SVM classifier trained on half the data, which sorted the remaining cluster identities into subtypes A and B with 100% accuracy. We next assessed responsiveness across epochs, as in Fig. 4, separately for neurons in the two subtypes.

Repeating the pairwise analyses performed on the total population (Fig. 4), we observed that each subtype expressed a unique set of response profiles exhibited at the population level (Fig. 5 B,C). Specifically, subtype A neurons demonstrated context dependence in the *priors* epoch (Fig. 5 B; $p = 0.0470$, 1-tailed t-test (paired), adjusted for multiple (n=5) comparisons; $p = 0.0102$, Cohen's $d = 0.709$, 1-tailed paired permutation test), while subtype B group showed context dependence in the *movement preparation* epoch (Fig. 5B; $p = 0.00382$, 1-tailed Wilcoxon signed rank test (paired), adjusted for multiple (n=5) comparisons; $p = 0.000645$, Cohen's $d = 0.323$, 1-tailed paired permutation test). When examining context dependence for ipsilateral movements (as in Fig. 4C), subtype A neurons showed an effect across all epochs but *movement preparation* (Fig. 5C; *priors*, $p = 0.0272$; *sensory processing*, $p = 0.0272$; *movement initiation*, $p = 0.0272$; *feedback*, $p = 0.0277$, 1-tailed t-test (paired) adjusted for multiple (n=5) comparisons; *priors*, $p = 0.0128$, Cohen's $d = 0.648$; *sensory processing*, $p = 0.0109$, Cohen's $d = 0.721$; *movement initiation*, $p = 0.0151$, Cohen's $d = -0.589$; *feedback*, $p = 0.0231$, Cohen's $d = -0.519$, 1-tailed paired permutation test), while subtype B neurons showed an effect only in the movement preparation epoch (Fig. 5C; $p = 0.0135$, 1-tailed Wilcoxon signed rank test (paired), adjusted for multiple (n=5) comparisons; $p = 0.00250$, Cohen's $d = 0.307$, 1-tailed paired permutation test).

Interestingly, for both subtypes, context-dependent responsiveness was always greater for patterned than unpatterned trials, as noted previously for the total population (Fig. 4B). Finally, during the feedback epoch, subtype A neurons showed outcome-dependent responsiveness (correct vs. incorrect) (Fig. 5D; $p = 0.0120$, 1-tailed t-test (paired) adjusted for multiple (n=5) comparisons; $p = 0.00173$, Cohen's $d = -0.995$, 1-tailed paired permutation test), while subtype B neurons did not (Fig. 5D; $p = 0.445$, 1-tailed Wilcoxon signed rank test). Together, these results demonstrate that subtypes A and B make complementary contributions to SNr function, with subtype A implicated in motor and non-motor task-relevant processes and subtype B playing a specialized role in motor preparation.

Discussion

This study examined whether SNr activity in PD patients contributed to changes in movement performance modulated by different contexts. We first assessed the dependence of behavioral performance on trial context (patterned vs. unpatterned) (Fig. 1D) and observed that the patterned context improved the speed (Fig.1E) and accuracy (Fig. 1F) of task performance. We then demonstrated, with independent methods (i.e., intraoperative assessment and post-hoc imaging), that recordings acquired during behavior were localized to the SNr (Fig. 2B), a region characterized by GABAergic projection neurons implicated in motor control [4 22]. Although this additional assessment resulted in exclusion of only 1 recording compared to the 24 which were dual confirmed to have been acquired in the SNr, we deem it a key assurance we have recorded from the SNr. Using thresholds established by Ramayya et al. in 2014 [12], we further identified the large majority of neurons as GABAergic (82%) with the remaining meeting partial criteria for GABAergic classification. While each of these methods (intraoperative assessment, post-hoc imaging reconstruction, and functional thresholding) are less reliable than post-mortem electrolytical lesioning, immunohistochemical analysis, or genetic phenotyping common in animal work, when taken together they form a new standard for validating intraoperative recordings and convincingly identify our recorded population as SNr GABAergic neurons.

We then investigated whether context, direction of response, or response outcome effected SNr activity of patients with PD. Epoch-based firing rate analyses (Fig. 3) revealed that context modulated SNr activity (n=33 neurons, Fig. 4A), specifically during events related to *sensory processing, movement preparation*, and *movement initiation*. For all epochs significantly modulated by context, changes in firing rate relative to baseline (i.e., responsiveness) were greater under the patterned compared to unpatterned conditions (Fig. 4A). One explanation for the increased responsiveness of SNr activity during patterned contexts, is that features of the patterned state (i.e., repeated actions, predictive priors) engage sensorimotor circuits that are adapted to quickly recognize and enact movement based on stable environments. While evidence for such differentially responsive parallel BG circuits has been previously described [24-26], our findings are the first to do so with direct recordings in humans. In addition, our results extend the scope of previous work focusing on alternate circuit activation in response to value assigned [27-30] to patterned and unpatterned contexts. Context dependent processing in the BG directly informs studies on value representation in BG, as well as studies of directional associations, sensorimotor processing,

and the importance of priors on informing upcoming decisions. Perhaps of greatest interest, our observations were made in PD patients, indicating that the responsiveness of BG output is retained despite significant loss of DA neurons [27]. One explanation is that the circuits activated by stable environments (i.e., patterned contexts) are relatively spared by PD neurodegeneration compared to circuits engaged by more unpredictable (i.e., unpatterned) conditions [31-33]. This interpretation is supported by our experimental observation of greater SNr responsiveness in the patterned context, although enhanced responsiveness could reflect greater recruitment of BG output in patterned compared to unpatterned contexts at baseline with equivalent neurodegeneration occurring in associated circuits.

Another key finding from our study pertains to the identification of two distinct subtypes (subtypes A & B, Fig. 5) from our SNr recordings. While our identification of subtypes within the SNr is a first using direct human recordings, further investigation is required to determine how these functional subtypes might inform our understanding of PD effected circuitry and related treatments. To place our subtype specific findings in a framework of BG activity, we have illustrated how each subtype may match with known projection targets based on their putative functional profile (Fig. 6). Given that subtype B neurons exhibited a contextually selective effect for the *movement preparation* epoch only, we posited these neurons project solely to the thalamus, as this projection is the largest and most clearly implicated in motor control [4 6 34 35]. The more heterogeneous responses of subtype A neurons suggest they likely project to regions that contribute to sensorimotor integration, such as the superior colliculus (SC), which is the second largest projection out of the SNr and is implicated in decision making [35-37]. The pedunculopontine tegmental nucleus (PPTg) fills a similar role as the SC and has been shown to represent recent choices in mice performing a similar, ethologically adapted version of the task used in our study [38 39], making it a likely target of subtype A neurons given their contextual selectivity in the *priors* epoch (Fig. 5B). While the above interpretations require additional research to further evaluate, specifically with intraoperative studies, they hint at pathways which may be leveraged to enhance the efficacy of neuromodulatory treatments. For example, directly modulating subtype B neurons may be particularly effective at attenuating bradykinesia. Subtype A neurons, seemingly tuned to both motor (Fig. 5C) and non-motor processes (Fig. 5B,C) may provide a mechanistic explanation for why patients with PD benefit from a contextually conducive environment on memory recall tasks [40].

Although these results further refine our understanding of PD BG function at the single neuron level, we must acknowledge the limitations of the experimental setting. Of note, the relatively small number of neurons which can be acquired with a conventional intraoperative paradigm suggest that follow-up studies be multi-site or deploy high density recording probes to aggregate larger sample sizes. Complementary electrophysiologic analyses focusing on local field potentials (LFP) are also of interest. In addition, to illustrate contextual related effects on BG output are robust, future studies should include more than one context-dependent task. In parallel with these formal follow-up studies, clinicians may be able to leverage advances in directional stimulation with chance placement of stimulatory probes near SNr output tracts to test whether stimulating specific tracts is linked to reproducible effects across patients as our framework predicts (Fig. 6). Caution is warranted in pursuing such endpoints, however, as adverse effects must be kept in mind. Nonetheless,

considering the potential gains in treatment efficacy, we believe further characterization and modulation of SNr is well supported.

Supplementary Material

Refer to Web version on PubMed Central for supplementary material.

Acknowledgments

We thank the study participants for graciously volunteering their time and energies, without which our work would not be possible. In addition, authors AT, GF, and JT thank co-authors and neurosurgeons Dr. Aviva Abosch and Dr. Stephen Ojemann for allowing use of their operating room, volunteering their time, and providing their support. We also thank Dr. Drew Kern, Dr. Pamela David-Gerecht, and Elizabeth Humes for assistance conducting our task in the operating room. In addition, thanks to Jacqueline Essig and members of the Felsen lab for providing valuable input on figure design.

Engineering support was provided by the Optogenetics and Neural Engineering Core at the University of Colorado Anschutz Medical Campus, funded in part by the National Institute for Neurological Disorders and Stroke of the National Institutes of Health under award number P30NS048154.

Funding:

This research was supported by funds from National Institutes of Health (R01NS079518, P30NS048154), the Boettcher Foundation's Webb-Waring Biomedical Research Awards program and the University of Colorado School of Medicine Center for NeuroScience.

References

1. Brown J, Pan WX, Dudman JT. The inhibitory microcircuit of the substantia nigra provides feedback gain control of the basal ganglia output. Elife 2014;3:e02397. doi: 10.7554/eLife.02397 [published Online First: 2014/05/23] [PubMed: 24849626]
2. McGregor MM, Nelson AB. Circuit Mechanisms of Parkinson's Disease. Neuron 2019;101(6):1042–56. doi: 10.1016/j.neuron.2019.03.004 [published Online First: 2019/03/22] [PubMed: 30897356]
3. Yelnik J, Francois C, Percheron G, et al. Golgi study of the primate substantia nigra. I. Quantitative morphology and typology of nigral neurons. J Comp Neurol 1987;265(4):455–72. doi: 10.1002/cne.902650402 [published Online First: 1987/11/22] [PubMed: 3123529]
4. Hikosaka O. GABAergic output of the basal ganglia. Prog Brain Res 2007;160:209–26. doi: 10.1016/S0079-6123(06)60012-5 [published Online First: 2007/05/15] [PubMed: 17499116]
5. Freeze BS, Kravitz AV, Hammack N, et al. Control of basal ganglia output by direct and indirect pathway projection neurons. J Neurosci 2013;33(47):18531–9. doi: 10.1523/JNEUROSCI.1278-13.2013 [published Online First: 2013/11/22] [PubMed: 24259575]
6. Kha HT, Finkelstein DI, Tomas D, et al. Projections from the substantia nigra pars reticulata to the motor thalamus of the rat: single axon reconstructions and immunohistochemical study. J Comp Neurol 2001;440(1):20–30. doi: 10.1002/cne.1367 [published Online First: 2001/12/18] [PubMed: 11745605]
7. Grillner S, Robertson B. The Basal Ganglia Over 500 Million Years. Curr Biol 2016;26(20):R1088–R100. doi: 10.1016/j.cub.2016.06.041 [PubMed: 27780050]
8. McGovern RA, Chan AK, Mikell CB, et al. Human substantia nigra neurons encode decision outcome and are modulated by categorization uncertainty in an auditory categorization task. Physiol Rep 2015;3(9) doi: 10.14814/phy2.12422 [published Online First: 2015/09/30]
9. Mikell CB, Sheehy JP, Youngerman BE, et al. Features and timing of the response of single neurons to novelty in the substantia nigra. Brain Res 2014;1542:79–84. doi: 10.1016/j.brainres.2013.10.033 [published Online First: 2013/10/29] [PubMed: 24161826]

10. Ramayya AG, Misra A, Baltuch GH, et al. Microstimulation of the human substantia nigra alters reinforcement learning. J Neurosci 2014;34(20):6887–95. doi: 10.1523/JNEUROSCI.5445-13.2014 [published Online First: 2014/05/16] [PubMed: 24828643]
11. Ramayya AG, Pedisich I, Levy D, et al. Proximity of Substantia Nigra Microstimulation to Putative GABAergic Neurons Predicts Modulation of Human Reinforcement Learning. Front Hum Neurosci 2017;11:200. doi: 10.3389/fnhum.2017.00200 [published Online First: 2017/05/26] [PubMed: 28536513]
12. Ramayya AG, Zaghloul KA, Weidemann CT, et al. Electrophysiological evidence for functionally distinct neuronal populations in the human substantia nigra. Front Hum Neurosci 2014;8:655. doi: 10.3389/fnhum.2014.00655 [PubMed: 25249957]
13. Zaghloul KA, Blanco JA, Weidemann CT, et al. Human substantia nigra neurons encode unexpected financial rewards. Science 2009;323(5920):1496–9. doi: 10.1126/science.1167342 [PubMed: 19286561]
14. Nieuwboer A, Kwakkel G, Rochester L, et al. Cueing training in the home improves gait-related mobility in Parkinson's disease: the RESCUE trial. J Neurol Neurosurg Psychiatry 2007;78(2):134–40. doi: 10.1136/jnnp.200X.097923 [PubMed: 17229744]
15. McIntosh GC, Brown SH, Rice RR, et al. Rhythmic auditory-motor facilitation of gait patterns in patients with Parkinson's disease. J Neurol Neurosurg Psychiatry 1997;62(1):22–6. [PubMed: 9010395]
16. Baram Y, Aharon-Peretz J, Badarny S, et al. Closed-loop auditory feedback for the improvement of gait in patients with Parkinson's disease. J Neurol Sci 2016;363:104–6. doi: 10.1016/j.jns.2016.02.021 [PubMed: 27000231]
17. Badarny S, Aharon-Peretz J, Susel Z, et al. Virtual reality feedback cues for improvement of gait in patients with Parkinson's disease. Tremor Other Hyperkinet Mov (N Y) 2014;4:225. doi: 10.7916/D8V69GM4 [PubMed: 24719779]
18. Arias P, Cudeiro J. Effect of rhythmic auditory stimulation on gait in Parkinsonian patients with and without freezing of gait. PLoS One 2010;5(3):e9675. doi: 10.1371/journal.pone.0009675 [PubMed: 20339591]
19. Tekriwal A, Felsen G, Thompson JA. Modular auditory decision-making behavioral task designed for intraoperative use in humans. J Neurosci Methods 2018;304:162–67. doi: 10.1016/j.jneumeth.2018.05.004 [published Online First: 2018/05/11] [PubMed: 29746889]
20. Liu D, Li W, Ma C, et al. A common hub for sleep and motor control in the substantia nigra. Science 2020;367(6476):440–45. doi: 10.1126/science.aaz0956 [published Online First: 2020/01/25] [PubMed: 31974254]
21. Rizzi G, Tan KR. Synergistic Nigral Output Pathways Shape Movement. Cell Rep 2019;27(7):2184–98 e4. doi: 10.1016/j.celrep.2019.04.068 [published Online First: 2019/05/16] [PubMed: 31091455]
22. Lintz MJ, Felsen G. Basal ganglia output reflects internally-specified movements. Elife 2016;5:e13833. doi: 10.7554/eLife.13833 [published Online First: 2016/07/06] [PubMed: 27377356]
23. Handel A, Glimcher PW. Quantitative analysis of substantia nigra pars reticulata activity during a visually guided saccade task. J Neurophysiol 1999;82(6):3458–75. doi: 10.1152/jn.1999.82.6.3458 [PubMed: 10601475]
24. Hikosaka O, Ghazizadeh A, Griggs W, et al. Parallel basal ganglia circuits for decision making. J Neural Transm (Vienna) 2018;125(3):515–29. doi: 10.1007/s00702-017-1691-1 [published Online First: 2017/02/06] [PubMed: 28155134]
25. Hanakawa T, Goldfine AM, Hallett M. A Common Function of Basal Ganglia-Cortical Circuits Subserving Speed in Both Motor and Cognitive Domains. eNeuro 2017;4(6) doi: 10.1523/ENEURO.0200-17.2017 [published Online First: 2018/01/31]
26. Kim HF, Hikosaka O. Parallel basal ganglia circuits for voluntary and automatic behaviour to reach rewards. Brain 2015;138(Pt 7):1776–800. doi: 10.1093/brain/awv134 [published Online First: 2015/05/20] [PubMed: 25981958]

27. Kim HF, Ghazizadeh A, Hikosaka O. Dopamine Neurons Encoding Long-Term Memory of Object Value for Habitual Behavior. Cell 2015;163(5):1165–75. doi: 10.1016/j.cell.2015.10.063 [published Online First: 2015/11/23] [PubMed: 26590420]
28. Kunimatsu J, Maeda K, Hikosaka O. The Caudal Part of Putamen Represents the Historical Object Value Information. J Neurosci 2019;39(9):1709–19. doi: 10.1523/JNEUROSCI.2534-18.2018 [published Online First: 2018/12/24] [PubMed: 30573645]
29. Choi Y, Shin EY, Kim S. Spatiotemporal dissociation of fMRI activity in the caudate nucleus underlies human de novo motor skill learning. Proc Natl Acad Sci U S A 2020;117(38):23886–97. doi: 10.1073/pnas.2003963117 [published Online First: 2020/09/10] [PubMed: 32900934]
30. Lau B, Glimcher PW. Value representations in the primate striatum during matching behavior. Neuron 2008;58(3):451–63. doi: 10.1016/j.neuron.2008.02.021 [PubMed: 18466754]
31. Gibb WR, Lees AJ. Anatomy, pigmentation, ventral and dorsal subpopulations of the substantia nigra, and differential cell death in Parkinson's disease. J Neurol Neurosurg Psychiatry 1991;54(5):388–96. doi: 10.1136/jnnp.54.5.388 [published Online First: 1991/05/01] [PubMed: 1865199]
32. Fearnley JM, Lees AJ. Ageing and Parkinson's disease: substantia nigra regional selectivity. Brain 1991;114 (Pt 5):2283–301. doi: 10.1093/brain/114.5.2283 [published Online First: 1991/10/01] [PubMed: 1933245]
33. Diederich NJ, Uchihara T, Grillner S, et al. The Evolution-Driven Signature of Parkinson's Disease. Trends Neurosci 2020;43(7):475–92. doi: 10.1016/j.tins.2020.05.001 [published Online First: 2020/06/06] [PubMed: 32499047]
34. Tanibuchi I, Kitano H, Jinnai K. Substantia nigra output to prefrontal cortex via thalamus in monkeys. I. Electrophysiological identification of thalamic relay neurons. J Neurophysiol 2009;102(5):2933–45. doi: 10.1152/jn.91287.2008 [published Online First: 2009/08/21] [PubMed: 19692504]
35. Parent A, Mackey A, Smith Y, et al. The output organization of the substantia nigra in primate as revealed by a retrograde double labeling method. Brain Res Bull 1983;10(4):529–37. doi: 10.1016/0361-9230(83)90151-x [published Online First: 1983/04/01] [PubMed: 6305462]
36. Wolf AB, Lintz MJ, Costabile JD, et al. An integrative role for the superior colliculus in selecting targets for movements. J Neurophysiol 2015;114(4):2118–31. doi: 10.1152/jn.00262.2015 [PubMed: 26203103]
37. Lintz MJ, Essig J, Zylberberg J, et al. Spatial representations in the superior colliculus are modulated by competition among targets. Neuroscience 2019;408:191–203. doi: 10.1016/j.neuroscience.2019.04.002 [published Online First: 2019/04/15] [PubMed: 30981865]
38. Thompson JA, Felsen G. Activity in mouse pedunculopontine tegmental nucleus reflects action and outcome in a decision-making task. J Neurophysiol 2013;110(12):2817–29. doi: 10.1152/jn.00464.2013 [PubMed: 24089397]
39. Thompson JA, Costabile JD, Felsen G. Mesencephalic representations of recent experience influence decision making. Elife 2016;5 doi: 10.7554/eLife.16572
40. Costa A, Monaco M, Zabberoni S, et al. Free and cued recall memory in Parkinson's disease associated with amnestic mild cognitive impairment. PLoS One 2014;9(1):e86233. doi: 10.1371/journal.pone.0086233 [published Online First: 2014/01/28] [PubMed: 24465977]

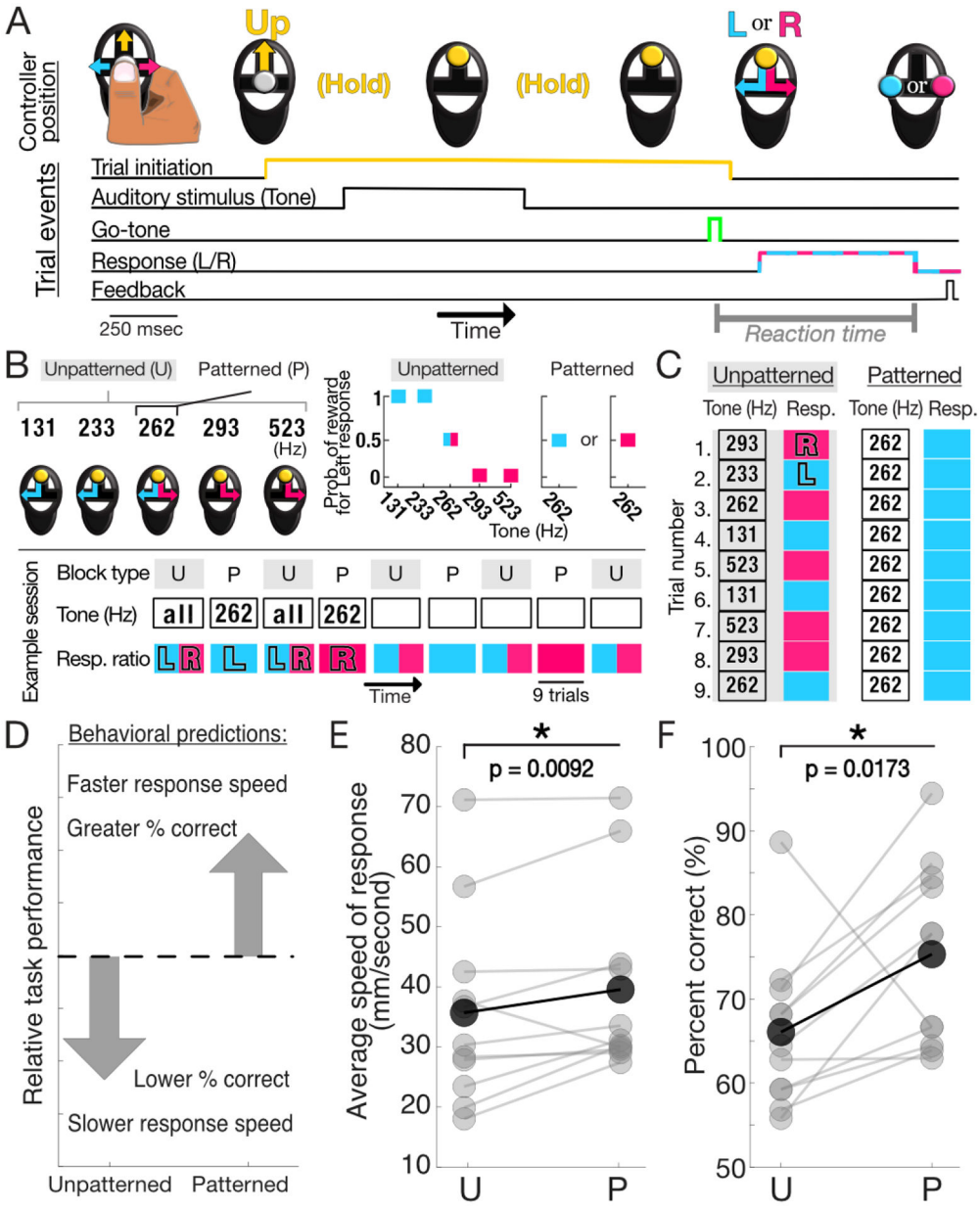

Figure 1: Task organization and behavioral findings.

A) Stereotyped interactions with handheld controller to elicit or respond to task events (top). Order and duration of task events (bottom). Dashed cyan-magenta line indicates that either the left (L, cyan) or right (R, magenta) movements are possible responses. **B)** (Top, left) All five auditory stimuli are presented in the unpatterned context while in the patterned context only the neutral tone stimulus (262Hz) is presented. Controllers depict possible correct choices for each tone: left for low pitch tones, right for high pitch tones, and either for the neutral tone. (Top, right) Probability of reward for a block of patterned or unpatterned trials following a left-sided response for each tone under the relevant contexts. Point represented by both magenta and cyan represent evenly split probability for leftward and rightward responses. (Bottom) Interleaved U (unpatterned) and P (patterned) block structure of a

typical session. During unpatterned blocks, presented stimuli include all tones with an equal proportion of L and R correct responses. During patterned blocks, only the 262Hz tone is presented and the rewarded side is fixed for the duration of the block. Note that left and right-sided responses are equally represented for both contexts across the entire session. **C)** Schematized representation of trial-by-trial comparison between unpatterned and patterned blocks. **D)** Task performance predicted to be enhanced during the patterned context relative to unpatterned. **E)** Within-session comparison of mean speed of response (i.e., time from go-tone until response detected) for U and P trials. Speed was significantly greater for P, as expected ($p = 0.0092$, 1-tailed Wilcoxon signed rank test (paired)). **F)** As in E, percent of trials correct significantly greater in P trials than U trials ($p = 0.0173$, 1-tailed two-sample t-test (paired))

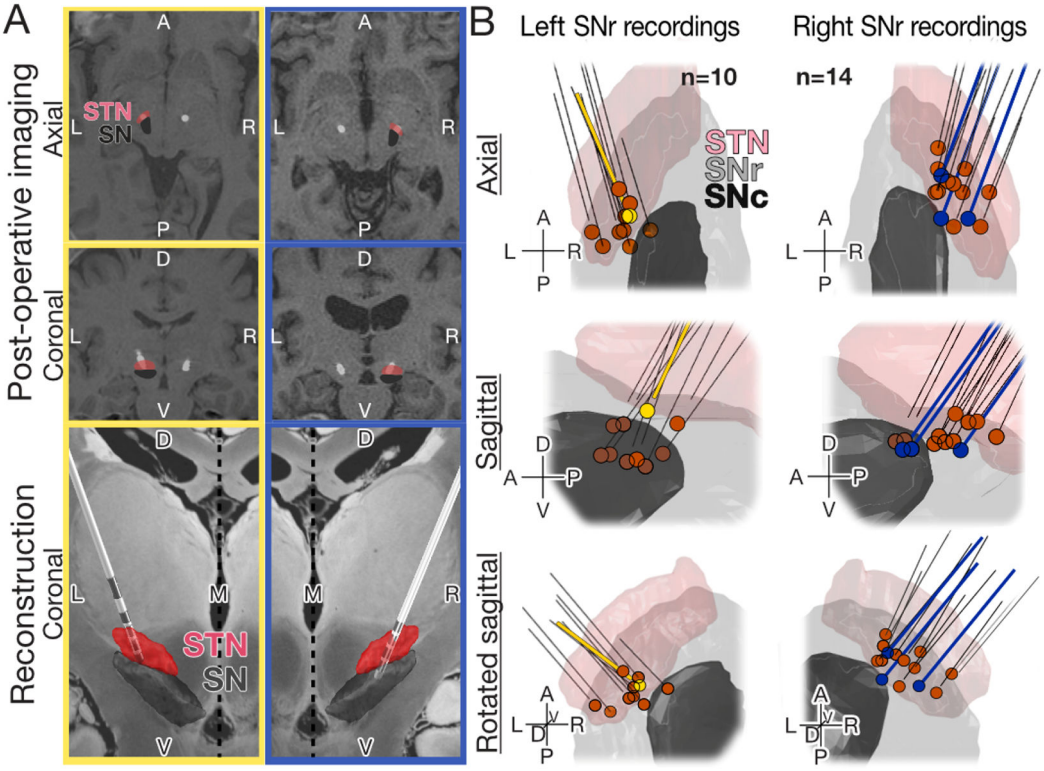

Figure 2: Post-hoc STN macroelectrode and SNr recording reconstruction

A) Post-surgical reconstruction of DBS lead placement for two representative cases (left, yellow; right, blue). Top two paired panels (top, coronal; middle, axial) demonstrate co-registered pre-operative MRI and post-operative CT (computed tomography). Representative cases demonstrate the variability in anatomy of patients with PD – note enlarged ventricular space for the second (blue) compared to first (yellow) case. Bottom paired panels are representative 3D reconstructions of the DBS lead with overlaid approximations of STN and SNr using Lead-DBS (Matlab, Supplementary Materials and Methods) showing placement within surgical target, the STN. Electrode configurations are representative of case specific hardware; Boston Scientific (yellow), Medtronic (blue) (Supplementary Materials and Methods). **B)** Reconstructive summary for all 24 recording (Supplementary Materials and Methods). Secondarily confirmed with post-surgical imaging (top: axial, middle: sagittal, bottom: rotated sagittal) to have occurred within the SNr, in support of expert clinical assessment at the time of surgery. Representative cases corresponding to A) are shown in yellow (left) and blue (right). Probe trajectories are represented by black lines; in cases where macroelectrode was implanted to same depth as the recording was acquired, the black line extends to the recording site (blue), whereas a gap reflects the offset between implant and recording depth (yellow). Supplementary Materials and Methods for a full description of post-hoc image analysis. Note that one of the 24 recordings was excluded from electrophysiologic analysis due to significant noise artifacts that could not be resolved with filtering.

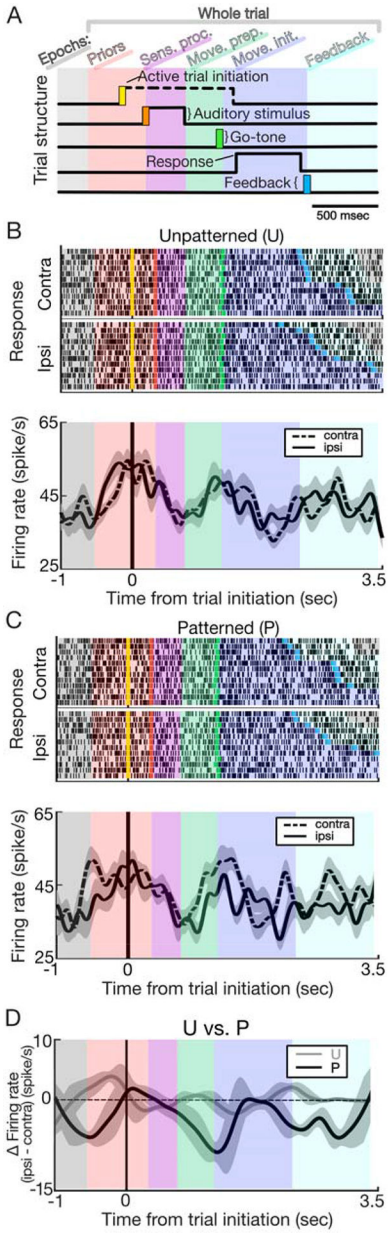

Figure 3: Representative SNr activity during task

A) Each trial consisted of five epochs (i.e., *priors, sensory processing, movement preparation, movement initiation*, and *feedback*) based on key task events. **B)** Rasters (top) and peri-event histograms (bottom) for an example neuron aligned to trial initiation (controller pressed 'Up') for unpatterned trials, separated by direction of response. Ipsilateral/contralateral is in relation to side of surgical intervention. Histograms are smoothed by taking the average firing rate in a moving 50ms window (shading, +/− 2 SEM (standard error of the mean)); note that y-axis does not extend to 0. Mean firing rates differ during *priors* and *movement initiation* epochs under the unpatterned context. **C)** As in B, but for the patterned context. All epochs but *sensory processing* differ in the patterned context. **D)** Comparing between contexts demonstrates that change in firing rate (firing rate during

trials in which ipsilateral movements are made – trials in which contralateral movements are made) is greater for the patterned context. All epochs but *sensory processing* differ between contexts. Histograms are smoothed by taking the average firing rate in a moving 200ms window (shading, +/− 2 SEM).

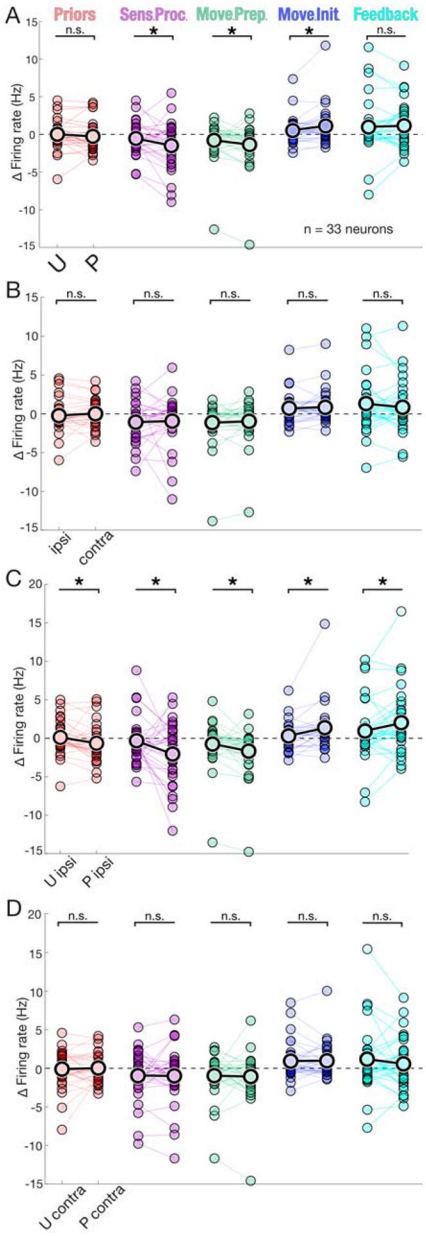

Figure 4: Context and condition dependent changes in SNr activity

A) Significant differences in selectivity between U (unpatterned) and P (patterned) contexts were found during *sensory processing, movement preparation*, and *movement initiation* epochs. *priors*, p = 0.100, Wilcoxon signed rank test; *sensory processing*, p = 0.0311*, Wilcoxon signed rank test; p = 0.0231*, Cohen's d = 0.364, permutation test; *movement preparation*, p = 0.0284*, Wilcoxon signed rank test; p = 0.0234*, Cohen's d = 0.220, permutation test *movement initiation*, p = 0.0284*, Wilcoxon signed rank test; p = 0.00376*, Cohen's d = −0.284, permutation test; *feedback*, p = 0.482, Wilcoxon signed rank test. Within session data comparisons are represented by connecting line, overall mean indicated by black outlined data points; n.s. (not significant), sens. proc. (sensory processing), move. prep. (movement preparation), move. init. (movement initiation). **B)** As in A) for ipsi.

(ipsilateral) compared to contra. (contralateral) responses, no significant differences found: *priors*, p = 0.322, Wilcoxon signed rank test; *sensory processing*, p = 0.322, Wilcoxon signed rank test; *movement preparation*, p = 0.344, Wilcoxon signed rank test; *movement initiation*, p = 0.322, Wilcoxon signed rank test; *feedback*, p = 0.322, Wilcoxon signed rank test. **C)** As in A) for U ipsi. compared to P ipsi. responses, significant differences found across all epochs;: *priors*, p = 0.00740*, Wilcoxon signed rank test; p = 0.0183*, Cohen's d = 0.333, permutation test; *sensory processing*, p = 0.0164*, Wilcoxon signed rank test; p = 0.0178*, Cohen's d = 0.484, permutation test; *movement preparation*, p = 0.00610*, Wilcoxon signed rank test; p = 0.00475*, Cohen's d = 0.327, permutation test; *movement initiation*, p = 0. 00610*, Wilcoxon signed rank test; p = 0.000615*, Cohen's d = −0.422, permutation test; *feedback*, p = 0.0164*, Wilcoxon signed rank test; p = 0.0250*, Cohen's d = −0.253, permutation test. **D)** As in A) for U contra. compared to P contra. responses, no significant differences found across any epochs: *priors*, p = 0.0805, Wilcoxon signed rank test; *sensory processing*, p = 0.0885, Wilcoxon signed rank test; *movement preparation*, p = 0.0885, Wilcoxon signed rank test; *movement initiation*, p = 0. 0885, Wilcoxon signed rank test; *feedback*, p = 0.0805, t-test. **(Not pictured)** As in A), for correct compared to incorrect responses, no significant differences found across any epochs: *priors*, p = 0.360, Wilcoxon signed rank test; *sensory processing*, p = 0.461, Wilcoxon signed rank test; *movement preparation*, p = 0.382, Wilcoxon signed rank test; *movement initiation*, p = 0. 382, Wilcoxon signed rank test; *feedback*, p = 0.0855, t-test. **(Note on statistics)** All reported t-test/Wilcoxon-tests p-values have been adjusted for multiple (n=5) comparisons, represent paired comparisons, and are 1-tailed. Permutation test results listed only for comparisons with significant t-test/Wilcoxon-tests and always performed with 100,000 iterations (Supplementary Materials and Methods).

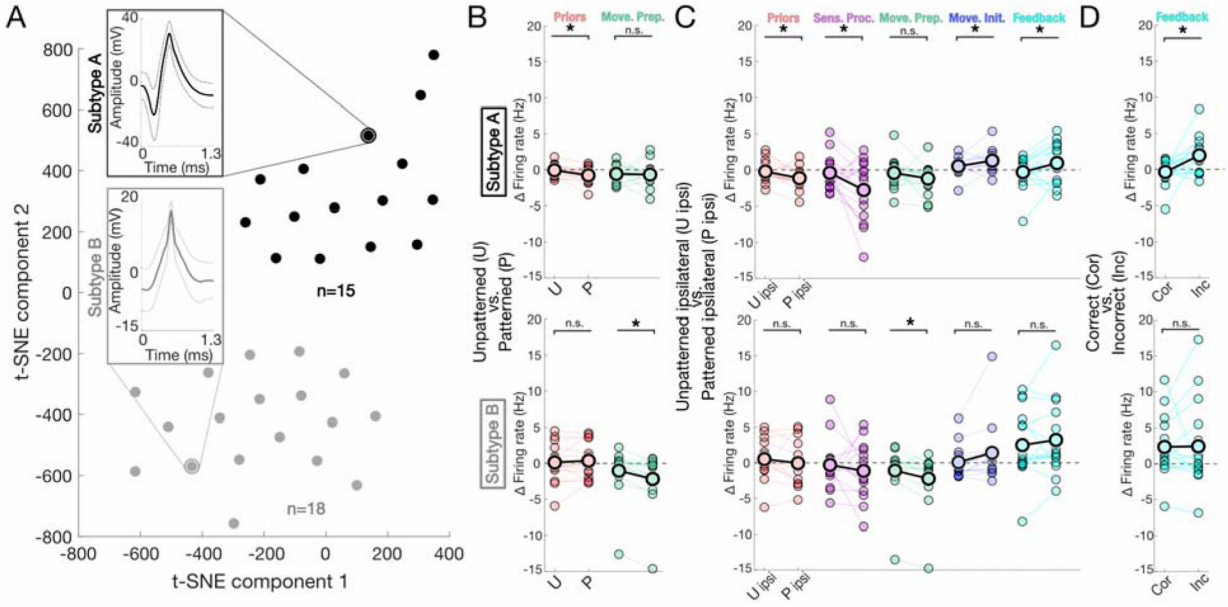

Figure 5: SNr subtypes and subtype-specific activity

A) Two clusters comprise the total population of recorded neurons as depicted by two-dimensional visualization of t-SNE. Cluster separation was assessed using two independent methods (k-means, DBSCAN, Supplementary Materials and Methods), as well as by an SVM classifier. **B)** Comparisons of epoch-specific firing rate changes between t-SNE determined subtype A (top) and subtype B (bottom) neurons. Plot title located alongside y-axis. Subtype A: *priors*, p = 0.0470*, t-test; p = 0.0102*, Cohen's d = 0.709, permutation test; *sensory processing*, p = 0.0780, Wilcoxon signed rank test; *movement preparation*, p = 0.416, t-test; *movement initiation*, p = 0.0565, t-test; *feedback*, p = 0.416, Wilcoxon signed rank test. Subtype B: *priors*, p = 0.333, t-test; *sensory processing*, p = 0.222, t-test; *movement preparation*, p = 0.00382*, Wilcoxon signed rank test; p = 0.000645*, Cohen's d = 0.323, permutation test; *movement initiation*, p = 0.222, Wilcoxon signed rank test; *feedback*, p = 0.481, t-test. Within session data comparisons are represented by connecting line, overall mean indicated by black outlined data points; n.s. (not significant), move. prep. (movement preparation) **C)** As in B) Subtype A: *priors*, p = 0.258, t-test; *sensory processing*, p = 0.262, Wilcoxon signed rank test; *movement preparation*, p = 0.0135*, Wilcoxon signed rank test; p = 0.00250 *, Cohen's d = 0.307, permutation test; *movement initiation*, p = 0.069, Wilcoxon signed rank test; *feedback*, p = 0.258, t-test. Subtype B: *priors*, p = 0.0272*, t-test; p = 0.0128*, Cohen's d = 0.648, permutation test; *sensory processing*, p = 0.0272*, t-test; p = 0.0109*, Cohen's d = 0.721, permutation test; *movement preparation*, p = 0.061, Wilcoxon signed rank test; *movement initiation*, p = 0.0272*, t-test; p = 0.0151*, Cohen's d = −0.589, permutation test; *feedback*, p = 0.0277*, t-test; p = 0.0231*, Cohen's d = −0.519, permutation test; sens. proc. (sensory processing), move. prep. (movement preparation), move. init. (movement initiation) **D)** As in B) Subtype A: *priors*, p = 0.138, t-test; *sensory processing*, p = 0.367, t-test; *movement preparation*, p = 0.0515, t-test; *movement initiation*, p = 0.367, t-test; *feedback*, p = 0.012*, t-test; p = 0.00173*, Cohen's d = −0.995, permutation test. Subtype B: *priors*, p = 0.445, Wilcoxon signed rank test; *sensory processing*, p = 0.200, Wilcoxon signed rank test;

movement preparation, p = 0.200, Wilcoxon signed rank test; *movement initiation*, p = 0.437, Wilcoxon signed rank test; *feedback*, p = 0.445, Wilcoxon signed rank test. **(Note on statistics)** All reported t-test/Wilcoxon-tests p-values have been adjusted for multiple (n=5) comparisons, represent paired comparisons, and are 1-tailed. Permutation test results listed only for comparisons with significant t-test/Wilcoxon-tests and always performed with 100,000 iterations (Supplementary Materials and Methods).

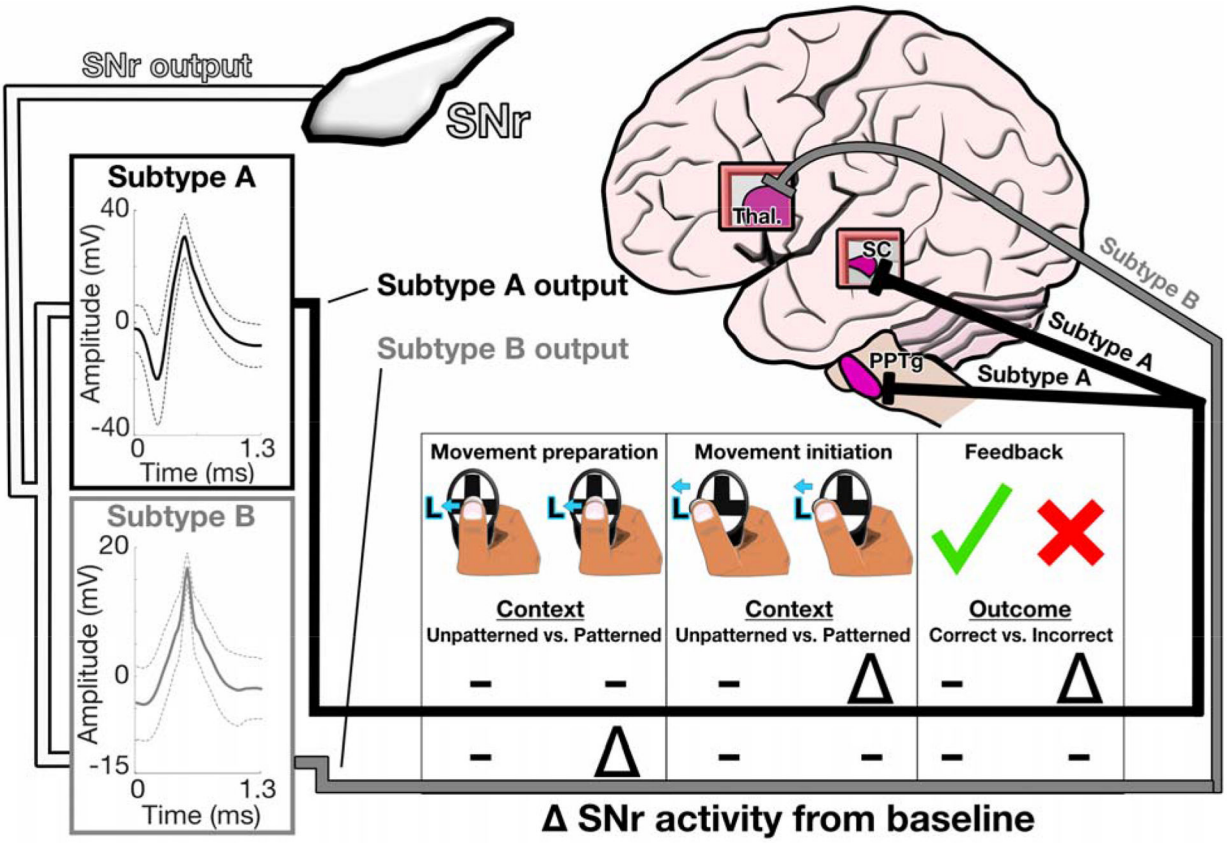

Figure 6: Proposed efferent targets from subtypes of SNr output neurons

Clustering of SNr neurons (n=33) based on waveform features revealed two distinct neuronal populations (subtype A, n = 15, black; subtype B, n = 18, grey). Key differences and similarities are illustrated for four distinct combinations of task epochs and responses. Projection targets for distinct subpopulations are a model for future work to expand upon.

Table 1:
Patient demographic, surgical, and symptom information.

Relevant information provided on a case-by-case basis. Patient #2 and #3 participated for both L (left) and R (right) STN surgical sessions while the remaining participated for one session. Dx (disease); LEDD (levodopa equivalent daily dose (mg)); UPDRS (Unified Parkinson's Disease Rating Scale).

Case #	Patient #	Target (R/L STN)	Handedness	Sex	Disease duration (years)	Age at time of study	PRE-LEDD	PRE ON UPDRS	PRE OFF UPDRS
1	1	R	Right	F	10	63	2692.5	20	47
2	2	R	Right	F	17	63	1128.75	11	43
3	2	L	Right	F	17	63	1128.75	11	43
4	3	L	Left	F	10	59	1143.75	19	42
5	3	R	Left	F	10	59	1143.75	19	42
6	4	R	Right	M	8	77	505	47	67
7	5	R	Right	M	12	67	1496.5	58	57
8	6	R	Right	M	9	70	1515	32	53
9	7	L	Right	M	8	54	1300	33	49
10	8	L	Right	F	8	66	660	16	30
11	9	L	Right	F	13	61	1755	7	33

R – right

L – left

LEDD – levodopa equivalent daily dose (mg)

UPDRS – Unified Parkinson's disease rating scale